Cavity control of active integrated antenna oscillators

M.Zheng, P.Gardener, P.S.Hall, Y.Hao, Q.Chen and V.F.Fusco

Abstract: The use of a cavity coupled to an active integrated antenna oscillator is described. The cavity increases the loaded Q factor of the oscillator, thus improving stability and reducing the phase noise. Cavity stabilisation of a microstrip patch and slot ring oscillators is described. In both cases, phase noise at a frequency offset of 10kHz is reduced by the order of 20dB. A first-order analysis based on measured and simulated cavity Q factors is shown to give similar results. A Van der Pol analysis of a two-element array of patch oscillators, with a single extended coupled cavity, indicates that the likelihood of mutual locking in an array which has oscillators with slightly different free running frequencies is enhanced albeit at the expense of increased start-up time.

1 Introduction

There has been a growing interest in integrating active three-terminal devices to passive planar antennas in recent years [1]. The applications of these active antennas are numerous and include spatial power combiners, distributed oscillator beam steering, low cost Doppler sensors and non-contact identification. However, because of their inherent radiation characteristics, active antenna oscillators normally have a relatively low Q factor and high single side-band (SSB) phase noise [2]. This is a serious deficiency, as oscillator noise is one of the limiting factors in many RF and microwave systems. For example, single sideband phase noise has a critical impact on the performance of Doppler radar systems. For Doppler radars to detect small cross-section targets in a clutter environment, low phase noise both in the transmitter and the receiver is necessary. Recently, with much wider use of phase and frequency modulation in telecommunication systems, the phase noise perturbations also have a pronounced degrading effect on the overall system performance. Several approaches can be taken to stabilise them. For example, injection locking can be used, but requires a separate stable source [3, 4]. Phase lock loop techniques can also be used [5, 6]. The issue of channelisation and communication capacity is also relevant. A phase lock loop allows simple frequency switching for use in a multichannel communication system. The use of cavity control fixes the frequency of operation. Some form of cavity tuning is then required to allow channel switching. This is not usually necessary in a radar application unless frequency hopping is needed. Cavity control also places a limit on the communication capacity or radar bandwidth and the trade-off between bandwidth and sensitivity, which may be determined by phase noise, is one of the important system design choices.

IEE Proceedings online no. 20010221

DOI: 10.1049/ip-map:20010221

Paper first received 20th March and in revised form 17th October 2000

M. Zheng, P. Gardener, P.S. Hall and Y. Hao are with the Communications Engineering Group, School of Electronic and Electrical Engineering, The University of Birmingham, Edgbaston, Birmingham B15 2TT, UK

Q. Chen and V.F. Fusco are with the High Frequency Electronics Laboratory, Department of Electrical and Electronic Engineering, The Queen's University of Belfast, Ashby Building, Stranmillis Road, Belfast BT9 5AH, UK

In this paper, the use of a coupled resonant cavity to reduce the phase noise of patch and slot loop antennas is presented. After discussing the importance of cavity quality factor to the oscillator phase noise and giving estimates based on measured Q factors, results for two cavity-backed active antenna oscillators are presented. The use of coupled cavity configurations is then shown to lead to improved oscillator locking properties, which has been acknowledged as a serious problem in large oscillator arrays.

2 Cavity Q factor

One of the most important factors under the control of active integrated antenna designers is the loaded Q of the oscillator. Typically Q_L is low because the oscillator is associated with a low Q antenna, whether it be a microstrip patch, slot or dipole antenna. Coupling of a cavity to the oscillator gives potential for increasing the loaded Q. The oscillator Q can also be increased by increasing the antenna Q. This can be done, for example, by the use of electrically thin substrates of high permittivity. However, this is unlikely to yield the potentially high Qs that can be obtained by the use of a high-quality cavity.

Loaded quality factor Q_L unloaded quality factor Q and external quality factor Q_e are defined as follows, assuming that the equivalent circuits of the patch and oscillator are parallel ones.

$$Q_e = R_L/\omega_0 L \tag{1}$$

$$\frac{1}{Q_L} = \frac{1}{Q_e} + \frac{1}{Q} \tag{2}$$

where R_L is the resistance of the loading circuit, L is the inductance of the circuit under consideration (i.e. patch antenna or oscillator) and ω_0 is the angular frequency.

In this Section, the cavity Q is assessed by a direct measurement of scattering parameters of an isolated cavity using a transmission method. A number of cavities are examined, including machined brass cavities at 4 and 34GHz and micromachined ones also operating at 34GHz with internal metallisation. In all cases, two small coaxial probes are mounted in a metal sheet that forms the top of the cavity. Loaded Q is determined from the measured S_{21} [7]. The accuracy of this measurement is believed to be of the order of ±10%. Table 1 gives results for the brass cavity at 4GHz, which was used for the oscillators described in Section 3.1

and 3.2, and for the 34GHz cavities. The calculated results were obtained from simulations using a finite element method (Hewlett-Packard high frequency structure simulator, HP-HFSS), modelling the measurement described above. The simulation included the effect of the sloping sides of the cavity.

Table 1: Measured and calculated loaded Q of cavities

Frequency (GHz)	Material	Measured	Calculated
4	brass	114	–
34	brass	808	1233
34	Cu film on HR-Si	340	2658
34	Al film on HR-Si	24	849

HR-Si = high resistivity silicon

The 34GHz cavities were constructed to demonstrate the likely performance of cavity controlled oscillators realised using silicon micromachining techniques. Cavities were produced by wet etching through-holes in the wafer, using thermally grown SiO_2 masks, augmented by LPCVD-TEOS, with a ternary mixture of KOH, IPA and DI-H_2O heated to 80°C. Such anisotropic etching of <111> float-zoned high resistivity silicon is produced through holes with 56° sloping edges. To obtain reasonable unloaded Q-factors at millimetre wavelengths, the depth of the cavity needs to be at least 2.0mm. As the standard silicon substrate thickness is only 625μm, several laminations are required. Pre-metallised laminations were glued together with conducting epoxy, using an alignment jig, as shown in Fig. 1.

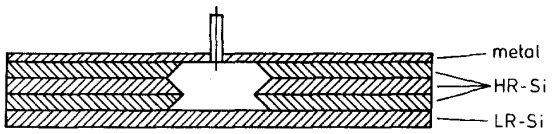

Fig. 1 *Millimetric cavity formed by laminated silicon wafers*

For cost reduction, the bottom lamination is formed using suitably metallised low resistivity silicon material. A metal top cap with co-axial probes was used in the measurement. A variety of techniques and metal types were used in order to establish a procedure that would result in good metallisation of the cavity walls. Evaporation and sputtering of gold, aluminium and copper was attempted. The use of gold was discounted, owing to the need for a titanium seed layer. Evaporated aluminium, 1.8μm thick, produced excellent results, giving 2.7μΩ cm resistivity and good adhesion. The low Q of 24 is [8] due to significant energy penetrating the walls and being lost as radiation [8]. A copper evaporation process was also developed, which yielded excellent 6.5μm thick layers having 1.7μΩ cm. A measured Q of 340 resulted. It is concluded that the Cu metallisation is superior for realising higher Q resonant structures, and that micromachined antenna oscillators with low phase noise can be realised using such techniques.

In general, Table 1 shows that calculated Q is higher than that measured, assumed to be because of mechanical imperfections in construction of the brass cavities and the use of adhesive in the micromachined ones. It is expected that improved micromachined cavities will result from the use of thermal bonding techniques.

3 Cavity-backed antenna oscillators

3.1 Cavity-backed patch oscillator

The 4GHz cavity-backed patch oscillator is shown in Fig. 2 [9]. The active patch oscillator was based on one previously published [10] and designed using the harmonic balance capability of the Hewlett-Packard microwave design system. The active antenna was made from glass-loaded PTFE substrate with a thickness of 0.508mm and a dielectric constant of 2.33. An AFT-26884 MESFET was mounted centrally on the edge of a 24 × 24mm square patch. The drain of the FET was connected to the centre of the patch side. The source and gate were separately connected to two 0.5mm width shortcircuited transmission lines with lengths of 5mm and 20mm, respectively. The ground plane of the patch antenna was attached to a brass cavity. A 1.5 × 30mm slot, 10mm away from the centre of the patch, was fabricated in the ground plane. The cavity was 50.5mm in width and 10mm in depth, its length could be varied by a slide plunger which was controlled by a micrometer drive. This arrangement would not be needed in a practical implementation. The TE_{101} cavity mode was excited by the slot, whose size and position were experimentally determined for optimum coupling.

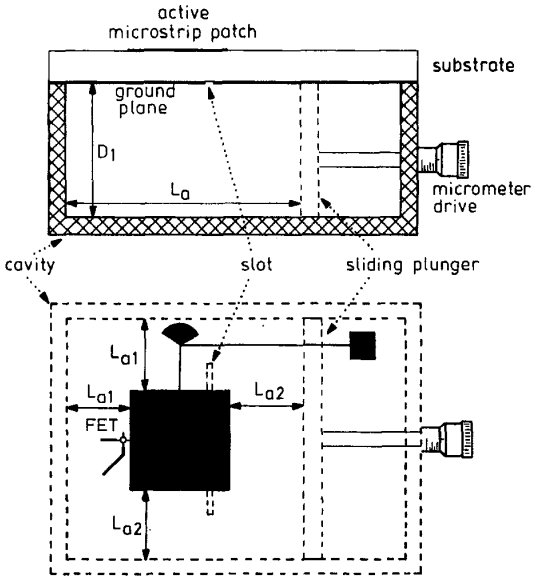

Fig. 2 *Microstrip patch oscillator with coupled resonant cavity*
D_1 = 10 mm, L_a = 54.8 mm, L_{a1} = 3.5 mm, L_{a2} = 27.3 mm, $L_{b1} = L_{b2}$ = 13.25mm, square patch's length = 24mm

Active patch antennas with and without the cavity were biased by a power supply (Hewlett-Packard-85671A) at 3 volts. A wide bandwidth antenna, 450mm away from the transmit antenna, was used to detect the radiated power. The active antenna noise was measured using a spectrum analyser (Hewlett-Packard-8563E) connected to the receive antenna. The spectrum analyser was controlled by a PC, *via* an IEEE-488 interface, to allow automatic data gathering.

The low Q active patch antenna oscillated at a frequency of 4.047GHz. After it was attached to the cavity, its frequency changed to 4.074GHz. To stabilise the oscillator, the cavity size was varied by adjusting the slide plunger. The spectrum of the received signal was monitored simultaneously. At a cavity length of 54.8mm, it was found that the noise of the active antenna oscillator was notably reduced. Simple calculation indicated that, at this length, the cavity's TE_{101} mode was resonant. The experimental results are presented in Figs. 3–5, which show the frequency spectrum and measured oscillator noise of the active antenna with and without the cavity, respectively. The noise measurement was performed using a direct spec-

trum method based on the Hewlett-Packard phase noise utility HP85671A [11]. From Fig. 5 it can be seen that the noise produced by the active patch antenna was significantly reduced by using the cavity

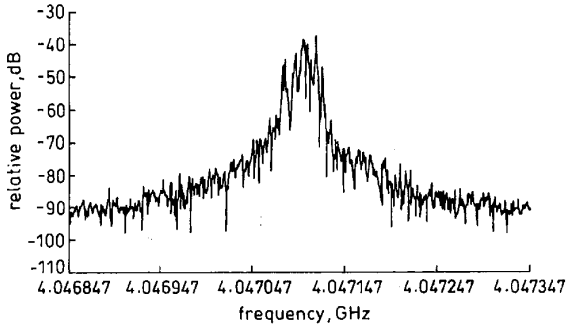

Fig. 3 *Signal spectrum of active patch oscillator without cavity*
Resolution bandwidth (RBW) = video bandwidth (VBW) = 3kHz

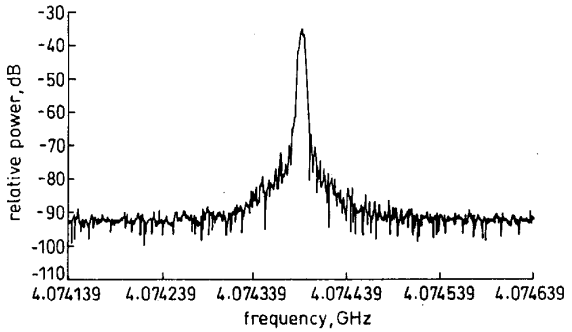

Fig. 4 *Signal spectrum of active patch antenna with cavity*
RBW = VBW = 3kHz

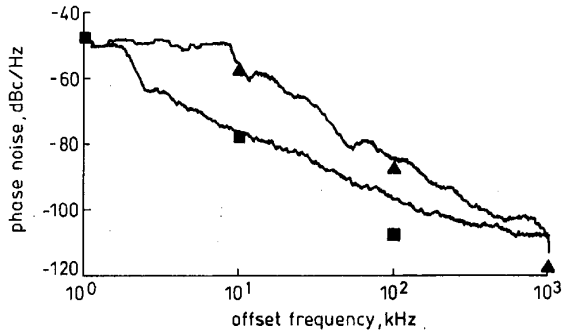

Fig. 5 *Phase noise of active patch antenna*
Lines and points; upper – without cavity, lower – with cavity
Lines – measured, points – calculated
Offset frequency is difference between phase noise measurement frequency and carrier frequency

3.2 Cavity-backed slot loop oscillator

The cavity-backed active slot loop antenna is shown in Fig. 6. The harmonic balance method, in conjunction with measured S parameters of a passive slot loop, was used to design the active slot loop antenna. The slot loop antenna had a length of 16.5mm and a width of 14.5mm was made from glass loaded PTFE substrate with a thickness of 0.508mm and a dielectric constant of 2.2. A low cost AFT-26884 MESFET was used and its drain and gate were separately connected to a 2.5mm and a 3mm long coplanar waveguide (CPW) line with a width of 1mm and a gap of 0.44mm; the former was further fed to the slot loop and the latter was shortcircuited at its end. The ground plane of the slot loop was attached to the brass cavity, which has a width of 50.5mm and a depth of 10mm. The slot loop and its ground plane formed the top wall of the cavity. It was anticipated that the TE_{101} cavity mode would be excited by the slot loop antenna, and an HP–HFSS simulation proved that this was the case.

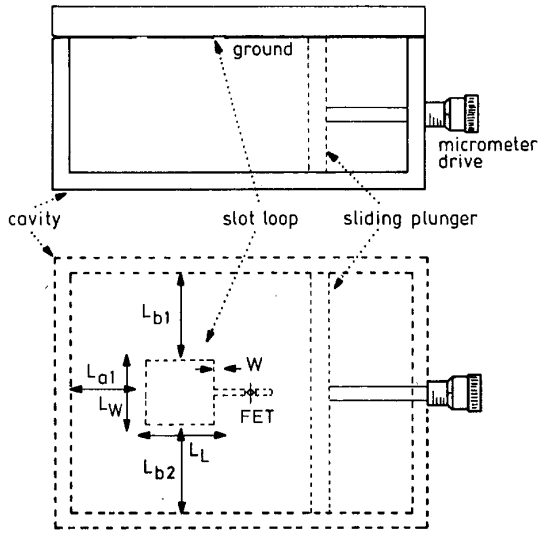

Fig. 6 *Cavity-backed active slot loop antenna*
L_{a1} = 30mm, $L_{b1} = L_{b2}$ = 18mm, L_W = 14mm L_L = 15mm and W = 1.5mm

The measurement arrangement was similar to that described in Section 3.1. The low Q active slot loop antenna oscillated at a frequency of 4.17GHz. After it was attached to the cavity, the frequency changed to 3.42GHz, and no attempt was made to adjust the oscillating frequency. It was found that, at a cavity length of 75mm, the oscillator noise of the active antenna was notably reduced. The experimental results are presented in Figs. 7–9, which show the frequency spectrum and measured oscillator noise of the active antenna, both with and without the cavity, respectively. From Fig. 9 it can be seen that

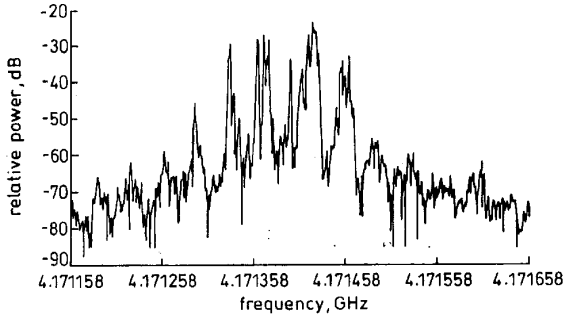

Fig. 7 *Signal spectrum of active slot loop antenna without cavity*
RBW = VBW = 3kHz, SPAN = 500kHz

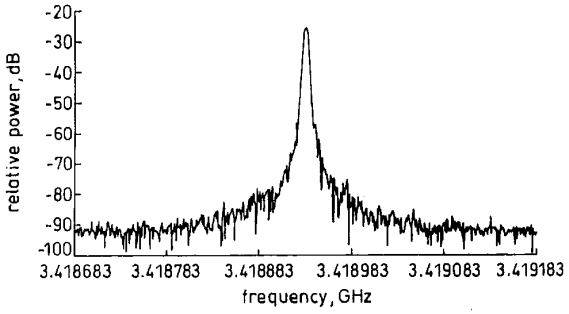

Fig. 8 *Signal spectrum of active slot loop antenna with cavity*
RBW = VBW = 3kHz, SPAN = 500kHz

the noise produced by the active slot loop antenna was reduced significantly by the use of the cavity. It can be observed that more than 30dB noise improvement was achieved at an offset frequency of around 40kHz. It was also found that the radiation power at the broad side was increased by approximately 3dB by attaching the cavity to the back of the active slot loop antenna.

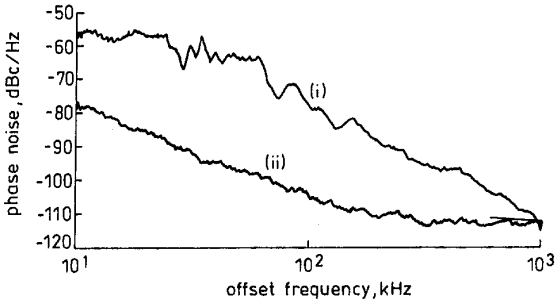

Fig. 9 *Measured oscillator noise of active slot loop antenna with and without a cavity*
(i) no cavity
(ii) cavity

3.3 Phase noise estimation from cavity Q

A good approximation to the single sideband noise spectral density L in an oscillator in dBc/Hz, is given by [12],

$$L(f_m) = \frac{1}{2}\left[1 + \frac{1}{f_m^2}\left(\frac{f_0}{2Q_L}\right)^2\right]\frac{FkT}{P_{av}}\left(1 + \frac{f_c}{f_m}\right) \quad (3)$$

where f_m is the offset frequency, F is the device noise factor at the operating frequency, kT is thermal noise (= –174dBm in a 1Hz bandwidth at room temperature), f_0 is the oscillator resonant frequency, f_c is the $1/f$ noise corner frequency of the device, P_{av} is the average output power and Q_L is the loaded Q of the oscillator.

For the case of the oscillator without the cavity, the Q factor is determined using the injection locking method. A signal close to the oscillator free running frequency is applied to the oscillator by injection through a small non-contacting coaxial probe, which has previously been characterised to allow the injected power to be determined. The locking bandwidth is determined by noting the frequencies at which lock is established and lost as the injected signal frequency is swept past the oscillator frequency. The external Q is given by [13],

$$Q_{ext} = \frac{kf_0}{\Delta f_{\max}}\sqrt{\frac{P_{inj}}{P_{av}}} \quad (4)$$

where k is a constant of order unity, f_0 is the oscillator frequency, Δf_{max} is the locking bandwidth and P_{inj} and P_{av} are the injected and oscillator powers, respectively. Measurement of the patch oscillator described in Section 3.1 without cavity resulted in Q = 9.8. The phase noise of the oscillator without the cavity is estimated from eqn. 3, with F = 3.0dB, T = 290K, P_{av} = 10mW, f_0 = 4GHz and f_c = 100MHz for a GaAs FET [14] and the result is shown in Fig. 5, compared to the measurement. It is noted that, at 10kHz offset frequency, the calculated value is –85dBc/Hz, whilst the measured value is –57dBc/Hz.

With the cavity attached, a loaded Q is calculated using equivalent circuit models of the coupled resonator structure, as shown in Fig. 11, where the parallel resonators are linked by a series conductance. The patch oscillator Q is as noted above (Q = 9.8) and the measured cavity Q is given in Table 1 as 114; the equivalent circuit component values are calculated from these Qs and first-order estimates of patch and cavity capacitances. The value of the coupling conductance is deduced from an HP–HFSS simulation of the structure and is 0.1 S. The resulting external Q of the coupled structure is 100.9. This Q is then used in eqn. 1 with other parameters as above. The result is compared with the measurement in Fig. 5. It can be seen that at 10kHz offset L = –78dBc/Hz; the measured value is –77dBc/Hz. The agreement between the calculated and measured values is thus seen to be good at this offset, although at higher frequencies this theory underestimates the noise.

To estimate the likely performance at millimetre wavelengths, the simulation using HP–HFSS of a 34GHz brass cavity was extended to include coupling to a patch antenna through a slot. This resulted in an external Q of 243. Eqn. 3 then gives a phase noise of –67.1dBc/Hz at a frequency offset of 10kHz and an improvement over an oscillator without a cavity of 28.7dB. As Table 1 indicates a lower Q from a silicon cavity, the phase noise improvement will be somewhat less than this.

4 Coupled cavity-backed oscillator arrays

The dynamic performance of the cavity-backed patch oscillator and two-element array of the form of Fig. 10 was investigated using a Van der Pol analysis of the equivalent circuit shown in Fig. 11. If the patch oscillator is used as an

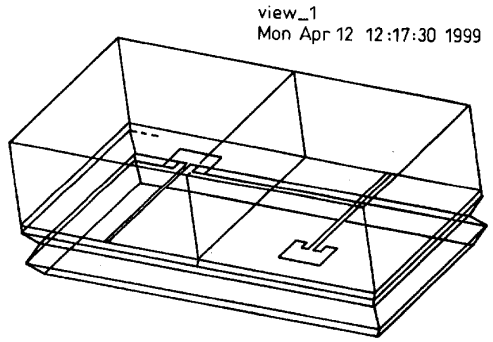

Fig. 10 *Two-element active antenna oscillator with coupled cavity backing*

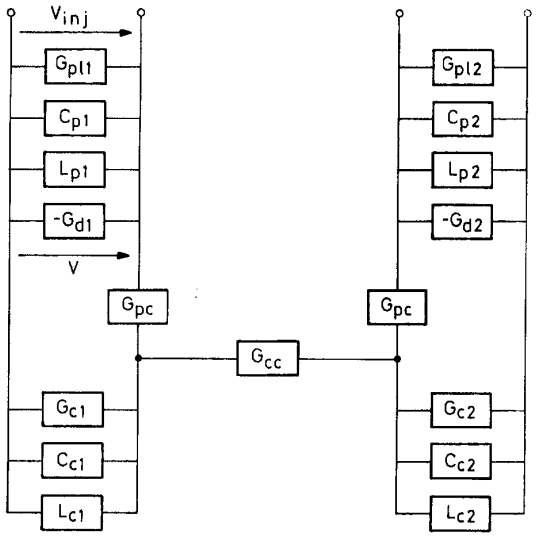

Fig. 11 *Equivalent circuit of two-element cavity-backed patch oscillator array*
C_p = 0.014pF, G_{p1} = 5.0mS, G_d = (20–10V) mS, C_c = 8.54pF, G_c = 5mS, $G_{pc} = G_{cc}$ = 0.1mS, L found from C for oscillation at 35GHz

element in a power combining array, improved coupling can be achieved with a pair of patches, slot coupled to cavities whose dividing wall has been removed to create a higher-order mode cavity. This gives high coupling between the oscillators and can be used to enhance mutual locking. Such mutual locking is a particular problem in large arrays, where the control of oscillator-free running frequency is degraded due to manufacturing tolerances.

In Fig. 11, subscript p and c relate to the patch oscillator and cavity, respectively, and G_{pc} and G_{cc} relate to the patch–cavity and cavity–cavity coupling, respectively. The patch oscillator is represented by a parallel tank circuit; $-G_d$ is a negative nonlinear conductance. An injection signal is applied to the first patch.

Analysis uses the method described by Stephan [15], in which four simultaneous differential equation are developed for the amplitude and phase of two coupled circuits. Two issues are examined. First C_p is varied to simulate the manufacturing variation in active device and oscillator production. Secondly, the start-up characteristics are studied.

To examine the performance of a single element, G_{cc} of Fig. 11 is put to zero. First, with no injection signal, the frequency of operation will change with C_p. For a 10% change, the operating frequency will change by 83kHz with the cavity and 158kHz without. If a 1mA injection current is applied, the element will operate at the design frequency, but with a phase error of 19° with the cavity and 25° without, for a 10% capacitance change. What is more significant is that the maximum capacitance change before lock is lost is increased from 12.1% to 17.3%, which corresponds to differences in the free running frequency between design and manufacture of 5.9% and 8.3% respectively. It is therefore concluded that the use of a cavity will improve the chances of element lock in practical arrays.

Fig. 12 shows the start-up characteristic of a single element with and without a cavity. It is observed that the time to steady state is increased by the addition of the cavity. The different steady-state voltage in each case is not significant; both oscillators will deliver approximately the same power.

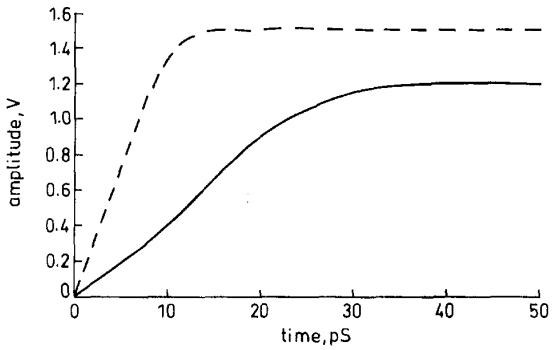

Fig. 12 *Calculated start-up characteristics of single patch oscillator*
– – – without cavity, ——— with cavity

The performance of the two element array shown in Fig. 10 has also been examined. The cavity to cavity coupling conductance G_{cc} was first determined by an HP–HFSS simulation. Then the four differential equations for the circuit of Fig. 11, with $G_{pc} = 0$, were solved to provide phase and amplitude of the two oscillator output voltages.

In operation, the signals from each oscillator are coupled to the other through the cavity, and in this way the two oscillators are mutually locked. In a large array, in which all the oscillators have slightly different free running frequencies due to manufacturing differences, it is important to determine whether locking can be achieved. This has been simulated here by varying C_{p2}, whilst holding C_{p1}, constant. The variation in C_{p2} before lock is lost was found to increase by 44% when coupling through the cavity was compared to coupling through mutual coupling between the patch antennas. This indicates that an array in which oscillators coupled by cavities will be much more tolerant of manufacturing differences.

Fig. 13 shows the start-up characteristics of the two-element array, modelled as above. Again, start-up time is increased by the addition of the cavity. Furthermore, comparison with Fig. 12 indicates that the array start-up time is considerably longer than for a single element. This is a consequence of the use here of a series feed type arrangement for the distribution of the locking signal, and similar conclusions as to the performance are drawn by Kykkotis [16]. This has implications for use in high bit rate communications applications, where a corporate type feed for distributing the locking signal to cavity-controlled elements may be more appropriate.

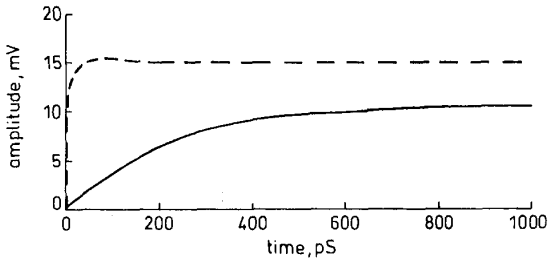

Fig. 13 *Calculated start-up characteristics of two-element array of patch oscillators*
– – – without cavity, ——— with cavity

5 Conclusions

This paper has explored the use of cavity coupling to stabilise active integrated antenna oscillators. Theoretical estimates for phase noise reduction have been supported by measured results for two types of active antennas. For both a patch oscillator and slot loop oscillator, phase noise improvements of the order of 20dB have been obtained. Furthermore, simulation using Van der Pol analysis has shown that cavity control gives increased tolerances to manufacturing errors in oscillator free running frequency in both single elements and arrays. The use of silicon micromachining may ultimately allow low cost production of power combining oscillator arrays that have an increased likelihood of mutual locking.

6 Acknowledgments

This work was performed as part of a joint project between The University of Birmingham and The Queen's University of Belfast. The project was supported by the UK Engineering and Physical Research Council (EPSRC) on grant GR/K 75682 and 75675. The authors would like to thank Dr M.J. Cryan for providing active patch antenna data and for many helpful discussions.

7 References

1 NAVARRO, J.A., and CHANG, K.: 'Active microstrip antennas' *in* LEE, K.F., and CHEN, W. (Eds.): 'Microstrip and printed antennas' (John Wiley, 1997), pp. 390–409
2 CHANG, H.-C., CAO, X., MISHRA, U., and YORK, R.A.: 'Phase noise in coupled oscillators: theory and experiment', *IEEE Trans.*, 1997, **MTT-45**, pp. 604–615
3 CHENG, K., HUMMER, K.A., and KLEIN, J.L.: 'Experiments on injection locking of active antenna elements for active phased arrays and spatial power combiners', *IEEE Trans.*, 1989, **MTT-37**, (7), pp. 1078–1084

4 CHANG, H.-C., CAO, X., VAUGHAN, M.J., MISHRA, U., and YORK, R.A.: 'Phase noise in externally injection locked oscillator arrays', *IEEE Trans.*, 1997, **MTT-45**, pp. 2035–2042
5 ANDREWS, J.W., and HALL, P.S.: 'Oscillator stability and phase noise reduction in phase lock active microstrip patch antenna', *Electron. Lett.*, 1998, **34**, (9), pp. 833–835
6 LYNCH, J.J., and YORK, R.A.: 'Mode locked arrays of coupled phase locked loops', *IEEE Microw. Guid. Wave Lett.*, 1995, **5**, (7), pp. 213–215
7 AITKEN, J.E.: 'Swept frequency microwave Q factor measurement', *IEE Proc.*, 1976, **123**, (9), pp. 855–862
8 WU, Y., CHEN, Q., FUSCO, V.F., ZHENG, M., and HALL, P.S.: 'Radiation leakage from an undermetallised silicon cavity'. IEEE MTT-S symposium, 1999, pp. 1331–1334
9 ZHENG, M., CHEN, Q., HALL, P.S., and FUSCO, V.F.: 'Oscillator noise reduction in a cavity-backed active microstrip patch antenna', *Electron. Lett.*, 1997, **33**, (15), pp. 1276–1277
10 CRYAN, M.J., and HALL, P.S.: 'Integrated active antenna with simultaneously transmit-receive operation', *Electron. Lett.*, 1996, **32**, (4), pp. 286–287
11 Hewlett Packard, User's Guide, HP85671A Phase Noise Utility, Part No. 85671–90010, 1994
12 LEESON, D.B.: 'A simple model of feedback oscillator noise spectrum', *Proc. IEEE*, 1966, **54**, pp. 329–330
13 KUROKAWA, K.: 'An introduction to the theory of microwave circuits' (Academic Press, New York, 1969), p. 388
14 SWEET, A.A.: 'MIC and MMIC amplifier and oscillator circuit design' (Artech House, Boston, 1943), p. 183ff
15 STEPHAN, K.D., and MORGAN, W.A.: 'Analysis of inter-injection-locked oscillators for integrated phased arrays', *IEEE Trans.*, 1987, **AP-35**, pp. 771–781
16 KYKKOTIS, C., HALL, P.S., and GHAFOURI-SHIRAZ, H.: 'Performance of active antenna oscillator arrays under modulation for communication systems', *IEE Proc., Microw. Antennas Propag.*, 1998, **145**, (4), pp. 313–320